

X-RAY DIFFRACTION STUDY OF THERMAL PROPERTIES OF
TITANIUM DIOXIDE

STANKO POPOVIĆ^a, ŽELJKO SKOKO^a, ANDREJA GAJOVIĆ^b,
KREŠIMIR FURIĆ^b and SVETOZAR MUSIĆ^b

^a*Physics Department, Faculty of Science, University of Zagreb, Bijenička cesta 32,
HR-10002 Zagreb, POB 331, Croatia*
E-mail addresses: spopovic@phy.hr, zskoko@phy.hr

^b*Ruđer Bošković Institute, POB 180, 10002 Zagreb, Croatia*

Dedicated to the memory of Professor Vladimir Šips

Received 31 January 2005; revised manuscript received 14 April 2005

Accepted 2 May 2005 Online 21 October 2005

Temperature dependence of microstructure of titanium dioxide, TiO₂, and the phase transition of anatase (**A**) to rutile (**R**) were studied by *in situ* X-ray powder diffraction. The as-synthesized TiO₂ p.a. showed a gradual transition **A**→**R** during the temperature increase from ≈ 1200 K to ≈ 1570 K and during the temperature decrease to ≈ 600 K. High-energy ball milling at room temperature induced a partial transition **A**→**R**. The transition continued during the temperature increase to ≈ 1370 K and during the temperature decrease, and is accompanied by sharpening of diffraction lines. Anisotropy of thermal expansion was noticed for both **A** and **R**. In the transition **A**→**R**, the nuclei of **R** are formed either throughout the **A** crystallites (in the case of as-synthesized TiO₂ p.a.) or mainly in the interior of the **A** crystallites (in the case of the milled TiO₂ p.a.). These nuclei grow in number and size with a prolonged time of thermal agitation.

PACS numbers: 61.50.Ks, 64.70.Kb, 65.40.De, 65.70

UDC 548.73

Keywords: titanium dioxide, rutile, anatase, phase transition, thermal expansion, X-ray powder diffraction

1. Introduction

Titanium dioxide, TiO₂, has been attracting attention of scientists for a long time because of its crystalline polymorphs. It is also an important traditional material in industry (e.g. white pigments, paints, cosmetics, pharmaceuticals) and in modern technology (e.g. solar cells, photovoltaic devices, optical filters, membranes,

gas and moisture sensors, catalysts) [1-5]. In recent years, a special attention has been paid to nanosized TiO₂, prepared for instance by the sol-gel procedure, and to thin films, prepared by the chemical vapour deposition or spray technique, as well as to TiO₂ doped with transition metal cations, in order to obtain favourable physical (optical, electrical, photocatalytic) properties [6-8].

Titanium dioxide, TiO₂, under a standard pressure and temperature, appears in nature in several crystal polymorphs: anatase [tetragonal, space group $I4_1/amd$ (141); unit-cell parameters at 25° C: $a = 3.784(2)$, $c = 9.514(5)$ Å (1 Å=0.1 nm); $Z = 4$; density 3.89 g/cm³ [9], PDF, e.g. card no. 78-2486], rutile [tetragonal, space group $P4_2/mnm$ (136); unit-cell parameters at 25° C: $a = 4.594(1)$, $c = 2.958(1)$ Å; $Z = 2$; density 4.25 g/cm³ [9], PDF, e.g. card nos. 87-0920, 86-0147], brookite [orthorhombic, space group $Pbca$ (61); unit-cell parameters at 25° C: $a = 9.19(2)$, $b = 5.46(1)$, $c = 5.15(1)$ Å; $Z = 8$; density 4.12 g/cm³ [9], PDF, e.g. card nos. 76-1937, 76-1934], high-pressure phase, TiO₂ II [orthorhombic, space group $Pbcn$ (60); unit-cell parameters at 25° C: $a = 4.515(6)$, $b = 5.497(5)$, $c = 4.939(5)$ Å, $Z = 4$; density 4.33 g/cm³ [9], PDF, e.g. card no. 84-1750].

The phase transition of anatase (**A**) to rutile (**R**) does not take place at a fixed temperature, and the data found in the literature are rather contradictory. For example, according to Ref. [10], the transition **A**→**R** is observed in the temperature interval from 670 K to 1270 K, while according to Ref. [11], it is very slow at temperatures below 1070 K. The temperature and kinetics of the transition **A**→**R** depend on the characteristics of the starting anatase, such as particle size (specific surface), the content and kind of impurities, deviation from stoichiometry, as well as on the atmosphere and pressure to which the material is exposed. Some impurities accelerate the transition **A**→**R** (e.g., transition metal cations, inducing formation of oxygen vacancies), while others have the opposite effect (e.g., chlorine, sulphite, fluorine interstitial ions). It is also well known that high-energy ball milling induces phase transitions in TiO₂ at lower temperatures, yielding nanosized particles [12, 13, 14]. The transition **A**→**R** is connected with a decrease of the specific volume (an increase of the density) for ≈ 9%.

The aim of the present work was to follow the phase transition **A**→**R** in TiO₂ p.a. by *in situ* X-ray powder diffraction (XRD). The temperature behaviour of the as-prepared TiO₂ p.a. was compared to that of the high-energy ball-milled TiO₂ p.a., as well as to that of the milled and pressed TiO₂ p.a. It was of interest to define molar fractions of **A** and **R** as a function of temperature. Also, *in situ* XRD measurements could provide data on a possible thermal expansion anisotropy of both **A** and **R**. In the present paper, preliminary results are given, while a more detailed study (by application of other methods such as TEM, HRTEM, SAED, Raman spectroscopy etc.) is needed in order to obtain a complete evidence on the phase transitions in TiO₂.

2. Experimental

A commercial titanium dioxide (Aldrich) in the form of powder of purity 99.9+% was used. X-ray powder diffraction (XRD) data at high temperature [from room

temperature (RT) to 1570 K] were collected by a Philips MPD 1880 diffractometer having a high-temperature attachment and a proportional detector, and using monochromatized $\text{CuK}\alpha$ radiation (monochromator: graphite). The temperature of the samples was increased/decreased at a rate of 3 to 4 K per minute. The air pressure in the high-temperature attachment was maintained at 10^{-2} Pa. Three experiments were performed: with (1) powder as-synthesized; (2) ball-milled powder; (3) ball-milled powder pressed in a form of thin pellet. The as-synthesized powder was milled for 10 hours in air, using a ball mill (vial and balls made of zirconium) and applying the powder-to-ball mass ratio of 1:10. The milled powder was pressed under a pressure of 0.18 GPa, which is several times smaller than the pressure necessary to induce the phase transition $\mathbf{A} \rightarrow \text{TiO}_2 \text{ II}$ [14]. A detailed description of the milling process is given in Ref. [14]. In all experiments, the heating/cooling run was stopped (for ≈ 15 min) at a series of temperatures in order to scan a characteristic part of the diffraction pattern.

The crystallite sizes were estimated from XRD line broadening using the Scherrer equation, after the correction for instrumental broadening. The molar fractions of \mathbf{A} and \mathbf{R} were found by comparison of the measured relative intensities of prominent diffraction lines of the two phases and the relative intensities calculated on the basis of the crystal structures.

3. Results and discussion

Characteristic parts of XRD patterns of the as-synthesized TiO_2 p.a. powder at RT, at 1573 K and again at RT, after a complete heating and cooling cycle, are shown in Fig. 1. The dominant phase at RT (before heating) was \mathbf{A} , while \mathbf{R} was present in traces (Fig. 1a). One can notice rather sharp diffraction lines due to big crystallites (estimated to 140 to 150 nm in size). During the heating run, the intensities of diffraction lines of anatase slowly decreased due to increased thermal vibrations of atoms. At the same time, diffraction lines shifted toward smaller

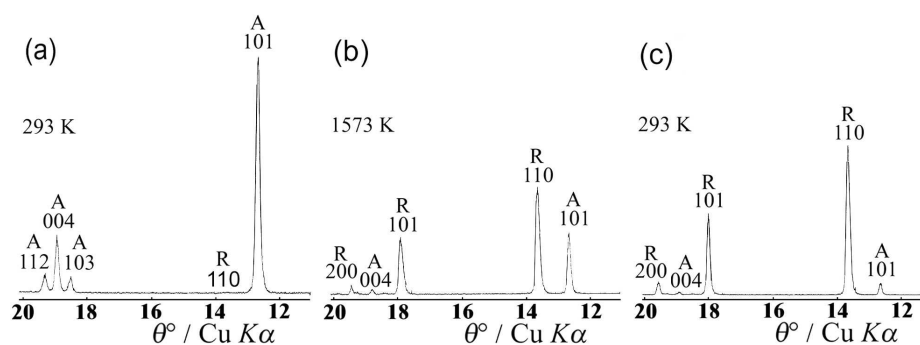


Fig. 1. Characteristic parts of XRD patterns of the as-synthesized TiO_2 at (a) RT, (b) 1573 K, (c) RT, after a complete heating and cooling cycle; \mathbf{A} = anatase, \mathbf{R} = rutile.

Bragg angles due to thermal expansion. It was found that thermal expansion of **A** was anisotropic. A very small increase in diffraction line widths with the increase of temperature was observed. Above ≈ 1200 K, a gradual transition **A**→**R** took place. At the highest temperature reached in this experiment, 1573 K, the fraction of **R** was bigger than that of **A** (Fig. 1 b). During the cooling run, the transition **A**→**R** continued and apparently ceased below ≈ 600 K. At RT, after cooling, the sample contained **R** as the dominant phase, with several molar percent of **A** (Fig. 1 c). **R** also exhibited an anisotropy in thermal expansion. The width of diffraction lines of both **A** and **R** depended very little on the temperature during the heating and cooling runs. The dependence of the molar fractions of **R** and **A** on temperature is shown in Fig. 2. Namely, in the present work, we concluded (on the basis of the literature data and our previous work) that the preferred orientation of crystallites

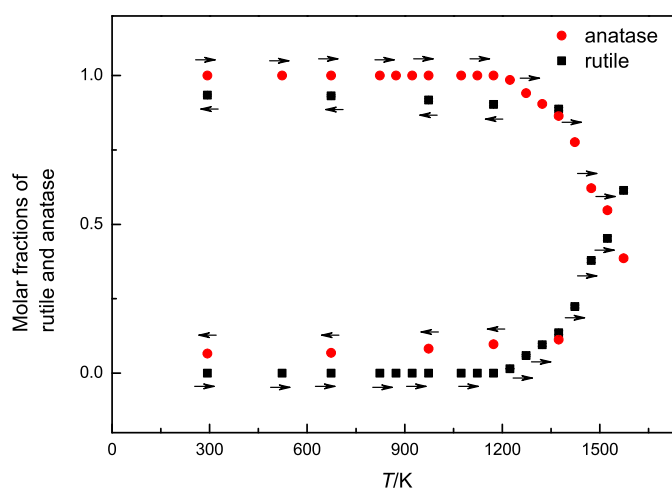


Fig. 2. The dependence of molar fractions of **A** and **R** on temperature of the as-synthesized TiO_2 during a complete heating and cooling cycle. The arrows indicate the sense of the temperature change.

in the sample was absent. Then, one can find the molar fractions of the phases present in the sample by comparison of the measured and calculated intensities of diffraction lines. For instance, by measuring the intensity of the rutile diffraction line 110, I_{100R} , and the intensity of the anatase diffraction line 101, I_{101A} , we found that the ratio of the molar fractions of rutile and anatase is given by the equation

$$\frac{R}{A} = 1.25 \frac{I_{100R}}{I_{101A}}.$$

The temperature dependence of the interplanar spacings d_{200} and d_{004} of anatase is shown in Figs. 3 and 4, respectively. The data in these figures are related to the heating run, where anatase was a dominant phase. From the data represented in Figs. 3 and 4, it followed that the average thermal expansion coefficients of anatase

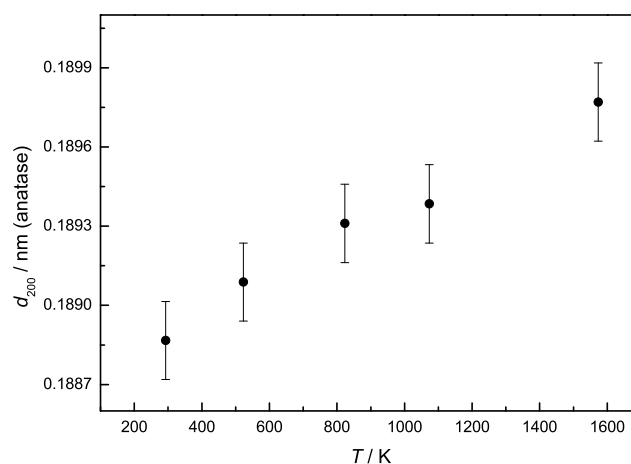


Fig. 3. The temperature dependence of the interplanar spacing d_{200} of anatase in the as-synthesized TiO_2 during the heating run. Vertical bars indicate e.s.d. in d_{200} .

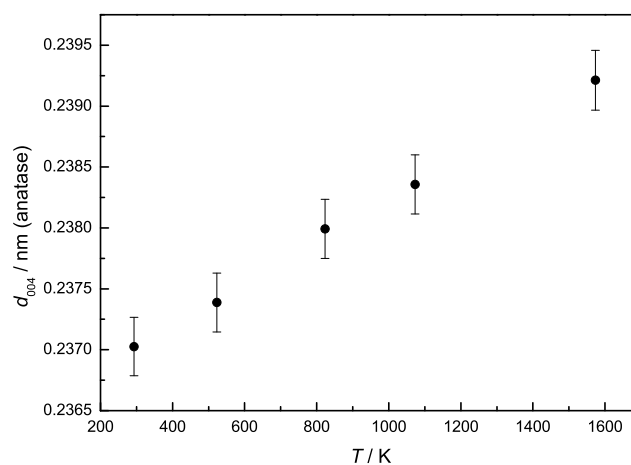


Fig. 4. The temperature dependence of the interplanar spacing d_{004} of anatase in the as-synthesized TiO_2 during the heating run. Vertical bars indicate e.s.d. in d_{004} .

(in the temperature interval from RT to ≈ 1570 K) amounted to $3.7(5) \times 10^{-6} \text{ K}^{-1}$ along the a -axis and $7.2(5) \times 10^{-6} \text{ K}^{-1}$ along the c -axis of the crystal lattice.

The temperature dependence of the interplanar spacings d_{110} and d_{101} of rutile is shown in Figs. 5 and 6, respectively. The data in these figures were collected in the cooling run, when rutile was a dominant phase. From the data on interplanar spacings of rutile, collected at various temperatures, the average thermal expansion

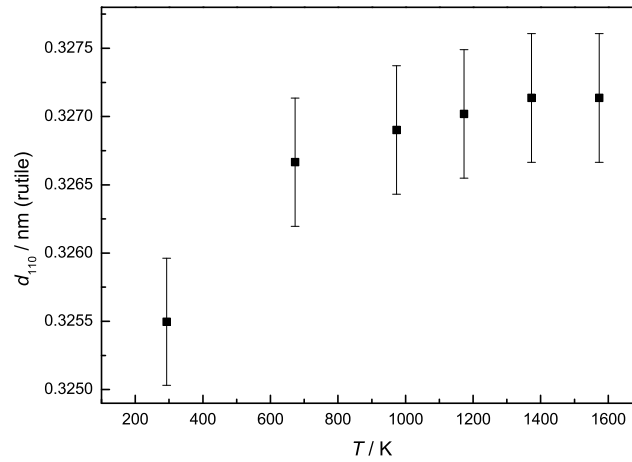


Fig. 5. The temperature dependence of the interplanar spacing d_{110} of rutile in the as-synthesized TiO_2 during the cooling run. Vertical bars indicate e.s.d. in d_{110} .

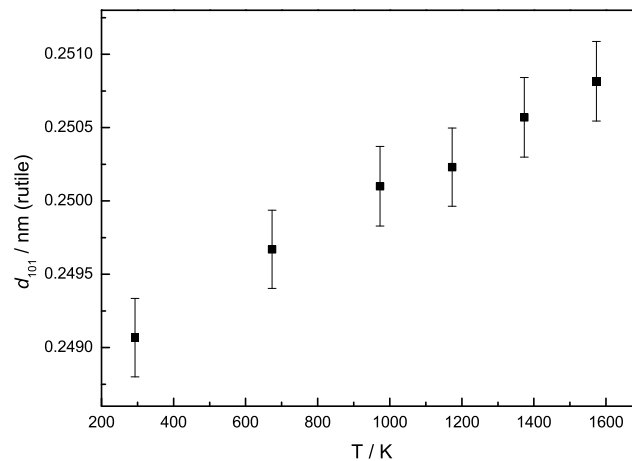


Fig. 6. The temperature dependence of the interplanar spacing d_{101} of rutile in the as-synthesized TiO_2 during the cooling run. Vertical bars indicate e.s.d. in d_{101} .

coefficients (in the temperature interval from ≈ 1570 K to RT) were found as follows: $4.1(5) \times 10^{-6} \text{ K}^{-1}$ along the a -axis and $6.0(6) \times 10^{-6} \text{ K}^{-1}$ along the c -axis.

The process of high-energy ball-milling of the as-synthesized TiO_2 induced the phase transitions $\mathbf{A} \rightarrow \mathbf{R}$, $\mathbf{A} \rightarrow \text{TiO}_2 \text{ II}$, or $\mathbf{A} \rightarrow \text{TiO}_2 \text{ II} \rightarrow \mathbf{R}$. The kinetics of the transitions was followed by XRD, Raman spectroscopy, transmission and scanning electron microscopy (TEM, SEM) and by selected-area electron diffraction (SAED). The details of that study are described elsewhere [14]. During 10 hours of milling, with the TiO_2 powder-to-ball ratio 1:10, the crystallite size decreased from some

150 nm to 12(3) nm. This fact was evidenced by XRD line broadening, as well as by TEM and SAED (electron diffraction pattern contained Debye rings instead of spots) [14]. The milling process also introduced lattice strains, which caused an additional broadening of XRD lines.

The phase composition of the TiO_2 , after 10 hours of milling, was as follows: **R** was the dominant phase, the molar fraction of **A** was ≈ 0.15 , and the molar fraction of TiO_2 II was ≈ 0.10 . Characteristic parts of XRD patterns of the milled TiO_2 powder at RT, at 1373 K and again at RT (after a complete heating and cooling cycle) are shown in Fig. 7. It is obvious from Fig. 7a that XRD lines were broadened, dominantly due to small crystallite sizes, as well as due to lattice strains. During heating, a sharpening of diffraction lines was noticed above ≈ 700 K. A transition of **A** (the fraction remained in the sample after milling) to **R** took place soon after the start of heating. At ≈ 1370 K (the highest temperature in this experiment) the sample contained only small amounts of **A** and TiO_2 II (Fig. 7 b). During the cooling run to RT, the sharpening of diffraction lines went on, due to a continuous increase of the crystallite size as well as an annealing of strains. During

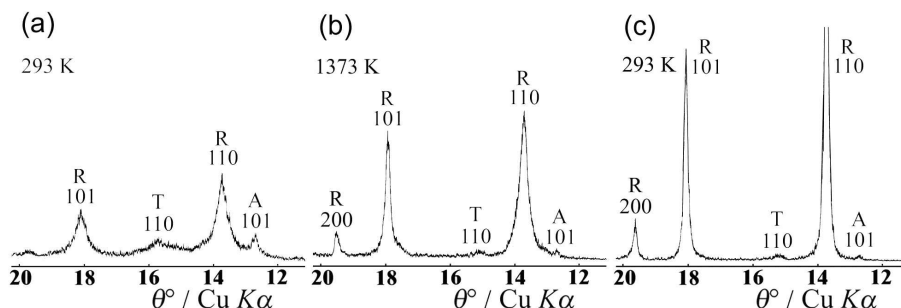


Fig. 7. Characteristic parts of XRD patterns of the high-energy ball-milled TiO_2 at (a) RT, (b) 1373 K, (c) RT, after a complete heating and cooling cycle; **A** = anatase, **R** = rutile, **T** = TiO_2 II.

the cooling run, the fraction of **R** continued to increase slowly, while the fractions of **A** and TiO_2 II decreased. At RT, after a complete heating and cooling cycle, XRD lines of **R** were as sharp as the ones of the non-milled sample (compare Fig. 7c and Fig. 1c). The fractions of **A** and TiO_2 II at RT were estimated from 0.02 to 0.03. The dependence of the molar fractions of **R** and **A** on temperature of the milled TiO_2 powder during a complete heating and cooling cycle is shown in Fig. 8. The data in this figure were plotted in terms of $\mathbf{A} + \mathbf{R} = 1$, i.e. fraction of TiO_2 II was not taken into account. Therefore, the phase transition $\mathbf{A} \rightarrow \mathbf{R}$, initiated by the milling process, was completed by thermal agitation of the sample.

The milled and pressed as-synthesized TiO_2 powder showed a dependence of the molar fractions of **R** and **A** on temperature similar to that of the milled sample. An overall thermal behaviour of this sample was more or less similar to that of the milled sample.

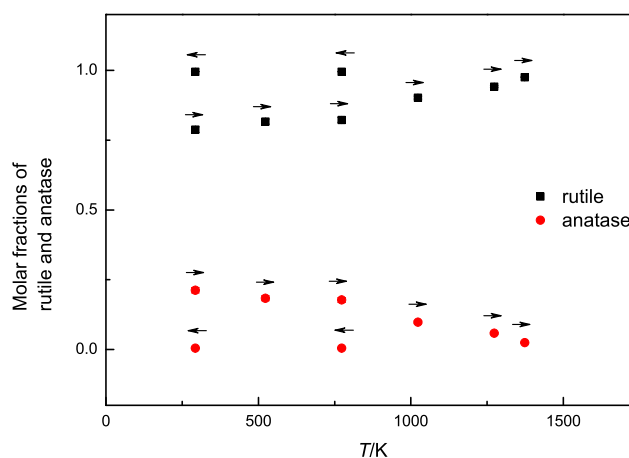


Fig. 8. The dependence of molar fractions of **A** and **R** on temperature of the high-energy ball-milled TiO_2 during a complete heating and cooling cycle. The arrows indicate the sense of the temperature change.

4. Conclusion

The phase transition anatase \rightarrow rutile (**A** \rightarrow **R**) in TiO_2 was followed by *in situ* X-ray powder diffraction (XRD). The experiments were performed with three samples: as-synthesized TiO_2 p.a., high-energy ball-milled TiO_2 p.a., the milled and pressed TiO_2 .

The as-synthesized TiO_2 p.a. was practically a single phase sample, containing **A**, showing sharp XRD lines due to big crystallites. On heating, the transition **A** \rightarrow **R** took place at a high temperature, above ≈ 1200 K; it continued to the highest reached temperature, ≈ 1570 K, but went on also during the cooling run, ceasing apparently below ≈ 600 K. According to the literature, in the transition **A** \rightarrow **R**, nuclei of **R** are formed both at the surface and in the interior of the **A** crystallites, and these nuclei grow in number and size with the increasing time of thermal agitation (Ref. [15] and the present work). **A** and **R** exhibited an anisotropy of thermal expansion.

High-energy ball-milling of TiO_2 p.a. induced the phase transition **A** \rightarrow **R**. After the milling process, the sample contained **R** as the dominant phase, and **A** and TiO_2 II as minor phases. XRD lines were broad due to small crystallite sizes and lattice strains due to the milling process. The transition of the remaining **A** and TiO_2 II (formed during milling) continued during the heating and cooling runs. At the same time, XRD lines became more and more sharp, as the crystallites grew and the lattice strains annealed. The transitions **A** \rightarrow **R** and $\text{TiO}_2\rightarrow$ **R** were also followed, for the same sample, by *in situ* Raman spectroscopy [14]. The Raman spectra at high temperatures, above ≈ 1200 K, showed no bands, due to the

high motion of oxygen vacancies and thermal electrons, breaking of Ti-O bonds and due to a possible reduction of Ti^{4+} [14]. On the other hand, XRD evidenced with certainty the presence of crystalline phases at high temperatures, because of a bigger penetration of X-rays in the particle interior. That indicates chemical and microstructural differences between the surface layer and the interior of TiO_2 particles in the milled sample. The comparison of Raman spectrometry [14] and XRD (the present work) might indicate that the phase transition $\mathbf{A} \rightarrow \mathbf{R}$ during milling started in the interior of TiO_2 particles, while the transition $\mathbf{A} \rightarrow TiO_2$ II, and then TiO_2 II $\rightarrow \mathbf{R}$, took place dominantly in the surface layers of the particles.

In order to obtain a more complete evidence in phase transitions in TiO_2 , additional studies, also by other methods, applied to different samples (varying in the particle sizes, distribution of particle sizes, preparation routes, impurity contents etc.) are necessary.

References

- [1] J. G. Balfour, in R. B. McKay, ed., *Technological Applications of Dispersion*, Marcel Dekker, New York (1994).
- [2] J. Moser, M. Grätzel and R. Gallay, *Helvetica Chimica Acta* **70** (1987) 1596.
- [3] B. O'Regan and M. Grätzel, *Nature* **353** (1991) 737.
- [4] J. K. Burdett, T. Hughbanks, G. J. Miller, J. W. Richardson and J. V. Smith, *J. Am. Chem. Soc.* **109** (1987) 3639.
- [5] J. F. Banfield, B. L. Bishoff and M. A. Anderson, *Chemical Geology* **110** (1993) 211.
- [6] S. Musić, M. Gotić, M. Ivanda, S. Popović, A. Turković, R. Trojko, A. Sekulić and K. Furić, *Mater. Sci. Eng. B* **47** (1997) 33.
- [7] A. M. Tonejc, M. Gotić, B. Gržeta, S. Musić, S. Popović, R. Trojko, A. Turković and I. Mušević, *Mater. Sci. Eng. B* **46** (1996) 177.
- [8] N. Šijaković-Vujičić, M. Gotić, S. Musić, M. Ivanda and S. Popović, *J. Sol-Gel Sci. Technol.* **30** (2004) 5.
- [9] *Powder Diffraction File*, Joint Committee on Powder Diffraction Standard, International Centre for Diffraction Data, Swarthmore, USA.
- [10] F. C. Gennari and D. M. Pasquevich, *J. Mater. Sci.* **33** (1998) 1571; *J. Am. Ceram. Soc.* **82** (1999) 1915.
- [11] J. M. Cviado, C. Real and J. Soria, *Solid State Ionics* **32/33** (1989) 461.
- [12] S. Begin-Colin, G. LeCaër, M. Zandona, E. Bouzy and B. Malaman, *J. Alloys and Comp.* **227** (1995) 157.
- [13] P. Bose, S. K. Pradhan and S. Sen, *Mater. Chemistry and Physics* **80** (2003) 73.
- [14] A. Gajović, K. Furić, N. Tomašić, S. Popović, Ž. Skoko and S. Musić, *J. Alloys Comp.* **398** (2005) 188.
- [15] A. R. West, *Solid State Chemistry and its Applications*, John Wiley and Sons, New York, 1984.

ISTRAŽIVANJE TERMIČKIH SVOJSTAVA TITAN DIOKSIDA
RENTGENSKOM DIFRAKCIJOM

Pomoću *in situ* rentgenske difrakcije u prahu, istraživali smo ovisnost mikrostrukture titan dioksida, TiO_2 o temperaturi i fazne pretvorbe anatasa (**A**) u rutil (**R**). Za polazni TiO_2 p.a. opaža se postepena pretvorba **A**→**R** pri porastu temperature od ≈ 1200 K do ≈ 1570 K, te pri smanjenju temperature do ≈ 600 K. Mljevenjem TiO_2 p.a. pri sobnoj temperaturi dolazi do djelomične pretvorbe **A**→**R**. Ta se pretvorba nastavlja pri porastu temperature do ≈ 1370 K, kao i pri smanjenju temperature, a prati je izoštravanje difrakcijskih linija. Uočena je anizotropija temperaturnog rastezanja za obje faze TiO_2 , **A** i **R**. Pri pretvorbi **A**→**R**, jezgre **R** nastaju ili u cijelom volumenu kristalita **A** (za polazni TiO_2 p.a.), ili uglavnom u unutarnjem dijelu kristalita **A** (za mljeveni TiO_2 p.a.). Veličina i broj jezgri **R** raste tijekom produljene termičke obrade uzorka.